THE JOURNAL OF BIOLOGICAL CHEMISTRY VOL. 290, NO. 26, pp. 16031–16042, June 26, 2015

Porphyromonas gingivalis-derived RgpA-Kgp Complex Activates the Macrophage Urokinase Plasminogen Activator System

*IMPLICATIONS FOR PERIODONTITIS**

Received for publication, February 12, 2015, and in revised form, May 12, 2015 Published, JBC Papers in Press, May 15, 2015, DOI 10.1074/jbc.M115.645572

Andrew J. Fleetwood[‡1], Neil M. O'Brien-Simpson[§], Paul D. Veith[§], Roselind S. Lam[§], Adrian Achuthan[‡], Andrew D. Cook[‡], William Singleton[§], Ida K. Lund[¶‖], Eric C. Reynolds[§], and John A. Hamilton[‡]

From the [‡]Department of Medicine, University of Melbourne, Royal Melbourne Hospital, Parkville, Victoria 3050, Australia, the [§]Oral Health Cooperative Research Centre, Melbourne Dental School, University of Melbourne, Victoria 3010, Australia, and the [¶]Finsen Laboratory, Rigshospitalet and the [‖]Biotech Research and Innovation Centre, Copenhagen University, 1165 Copenhagen, Denmark

Background: We recently found that uPA$^{-/-}$ mice are resistant to experimental periodontitis following oral infection with *P. gingivalis.*
Results: *P. gingivalis*-derived RgpA-Kgp complex activates the macrophage urokinase plasminogen activator.
Conclusion: *P. gingivalis* activates a critical host proteolytic pathway to promote tissue destruction.
Significance: A new host-pathogen interaction may promote tissues destruction and pathogen virulence in periodontitis.

Urokinase plasminogen activator (uPA) converts plasminogen to plasmin, resulting in a proteolytic cascade that has been implicated in tissue destruction during inflammation. Periodontitis is a highly prevalent chronic inflammatory disease characterized by destruction of the tissue and bone that support the teeth. We demonstrate that stimulation of macrophages with the arginine- and lysine-specific cysteine protease complex (RgpA-Kgp complex), produced by the keystone pathogen *Porphyromonas gingivalis*, dramatically increased their ability to degrade matrix in a uPA-dependent manner. We show that the RgpA-Kgp complex cleaves the inactive zymogens, pro-uPA (at consensus sites Lys^{158}-Ile^{159} and Lys^{135}-Lys^{136}) and plasminogen, yielding active uPA and plasmin, respectively. These findings are consistent with activation of the uPA proteolytic cascade by *P. gingivalis* being required for the pathogen to induce alveolar bone loss in a model of periodontitis and reveal a new host-pathogen interaction in which *P. gingivalis* activates a critical host proteolytic pathway to promote tissue destruction and pathogen virulence.

Urokinase plasminogen activator (uPA)[2] activates plasminogen to plasmin in a major proteolytic cascade that is involved in extracellular matrix degradation, fibrinolysis, and latent metalloproteinase activation (1, 2). Thus the uPA proteolytic cascade has been implicated in a number of diverse biological processes such as matrix remodeling, wound repair, inflammation, and tumor cell invasion (3, 4). We have previously found that uPA can be made by many cell types present in arthritic joints, including macrophages (5), and uPA levels in the synovium of rheumatoid arthritis patients correlate with disease severity (6, 7). Additionally, we have shown that uPA regulates macrophage motility and matrix degradation (8) and found a dependence on uPA for arthritis development in three systemic mouse models (9, 10).

uPA is produced as an inactive single-chain protein, pro-uPA, which is activated to its two-chain form by plasmin (11). In a positive-feedback loop, activated uPA cleaves the zymogen plasminogen to form plasmin, which is a broad spectrum serine protease (11). More specifically, plasmin cleavage of the zymogen pro-uPA at the Lys^{158}-Ile^{159} bond yields an A-chain and the protease domain-containing B-chain of active uPA, which are linked by an interchain disulfide bond (11, 12). Pro-uPA is also cleaved by plasmin at Lys^{135}-Lys^{136} to produce low molecular weight (LMW)-uPA and the N-terminal fragment (2, 13). At a molecular level, plasminogen, which circulates at high levels in the serum (14), is cleaved at the Arg^{561}-Val^{562} bond by uPA to produce the active two-chain plasmin. Active plasmin is comprised of a heavy and light chain held together by a disulfide bond (2, 11). Importantly, the uPA receptor (uPAR) localizes the activation of pro-uPA to the cell surface facilitating pericellular proteolysis of the extracellular matrix (4, 15).

Periodontitis (PD) is an infection-driven inflammatory disease typified by degradation of periodontal tissue, resorption of alveolar bone, and eventual tooth loss (16, 17). There are several bacterial species associated with PD (18), in particular *Porphyromonas gingivalis*, which is the species most strongly associated with various clinical indicators of PD (19). *P. gingivalis* has recently been described as a keystone pathogen for its ability to

* This work was supported by grants from the National Health and Medical Research Council of Australia (to J. A. H.). The authors declare that they have no conflicts of interest with the contents of this article.
[1] To whom the correspondence should be addressed: Dept. of Medicine, University of Melbourne, Royal Melbourne Hospital, Parkville, Victoria 3050, Australia. Tel.: 61-3-8344-3299; E-mail: andrew.fleetwood@unimelb.edu.au.
[2] The abbreviations used are: uPA, urokinase plasminogen activator; uPAR, uPA receptor; LMW, low molecular weight; PD, periodontitis; RgpA-Kgp complex, arginine- and lysine-specific cysteine protease complex; M-CSF, macrophage colony-stimulating factor; BMM, bone marrow-derived macrophage; MDM, monocyte-derived macrophage; TRITC, tetramethylrhodamine isothiocyanate; PAI-1, plasminogen activator inhibitor-1.

induce dysbiosis by targeting the host complement cascade, evading immune clearance and promoting destructive periodontal inflammation (20, 21).

Major virulence factors produced by *P. gingivalis* are the trypsin-like cysteine proteinases called gingipains (22). The gingipains comprise the arginine-specific (RgpA and RgpB) and the lysine-specific (Kgp) proteinases based on their ability to cleave Arg-Xaa or Lys-Xaa peptide bonds, respectively (22). RgpA and Kgp form an extracellular cysteine protease complex (RgpA-Kgp complex) common to all characterized *P. gingivalis* strains and is a major factor contributing to its pathogenicity (23, 24). The proteolytic activity of the gingipains enables *P. gingivalis* to degrade a range of host proteins including cytokines (*e.g.* IL-4, IL-12, and IFNγ), cell surface receptors (*e.g.* CD2, CD4, and CD14) and matrix proteins (*e.g.* fibrin, fibrinogen) (25). The peptides produced from such breakdown provide *P. gingivalis* with the nutrients it requires for growth and survival (18). Not only do the gingipains degrade host proteins, they also activate host systems, most notably the complement cascade, which enables *P. gingivalis* to subvert the host immune response and drive PD (20, 21).

uPA has been detected in inflamed periodontal tissue (26) and gingival crevicular fluid (27). Additionally, polymorphisms in the genes for uPA and one of its inhibitors have been associated with periodontal bone loss (28). However, the role of uPA in PD has not been defined. We recently found that $uPA^{-/-}$ mice are resistant to experimental PD following oral infection with *P. gingivalis*, possibly via a macrophage-dependent mechanism(s) (29). In agreement with that study, we also showed that depletion of macrophages, which can be a major source of uPA in inflammation (30), protected mice from *P. gingivalis*-induced PD (31) and that uPA regulates macrophage-mediated matrix degradation (8), a hallmark of chronic PD (16, 17). Therefore, in this study, we investigated the interaction of *P. gingivalis*-derived RgpA-Kgp complex with the uPA/plasminogen pathway in macrophages.

Experimental Procedures

Mice—Female C57BL/6 mice (6–8 weeks) were from Monash University (Malvern East, Australia) (32). The uPA gene-deficient mice ($uPA^{-/-}$) from Dr. P. Carmeliet (University of Leuven, Leuven, Belgium) were backcrossed onto the C57BL/6 background for 11 generations. The protocols used in this document were approved by the University of Melbourne Ethics Committee for Animal Experimentation (approval number 081049) and were conducted in accordance with the Declaration of Helsinki. All human blood donors gave written informed consent.

Reagents—The reagents were as follows: recombinant human macrophage-colony stimulating factor (M-CSF) (Chiron, Emeryville, CA); human pro-uPA was a kind gift from Novo Nordisk A/S (Copenhagen, Denmark); human glu-plasminogen (Enzyme Research Lab, South Bend, IN); human plasmin (Calbiochem), uPA and PAI-1 (Molecular Innovations, Novi, MI), and α2-antiplasmin (Innovative Research, Novi, MI); anti-human uPA mAb (clone U-16; Thermo Scientific, Waltham, MA); anti-mouse uPA mAb (clone mU1, Finsen Laboratory, Copenhagen, Denmark) (33); and mouse IgG1 (MOPC-21; BioXcell, West Lebanon, NH). Chromogenic substrates S2444 and S2251 were from Chromogenix (Mölndal, Sweden).

Bacterial Strains, Growth Conditions, and Purification of the RgpA-Kgp Complexes—*P. gingivalis* strain W50 (ATCC 53978) was grown and harvested as before (34). The purification of the RgpA-Kgp complexes was performed as before (35) and were activated prior to use with 10 mM L-cysteine in 0.5 M Tris/HCl, pH 7.4 buffer.

Preparation of Mouse Bone Marrow-derived Macrophages (BMM) and Human Monocyte-derived Macrophages (MDM)—Murine BMM and human MDM were prepared as before (36). Bone marrow cells from the femurs of mice were cultured in RPMI 1640 medium with 10% FCS, 2 mM GlutaMAX-1, 100 units/ml penicillin, 100 μg/ml streptomycin, and M-CSF (2000 units/ml). On day 7, adherent cells were harvested. Human monocytes were purified from buffy coats (Red Cross Blood Bank, Melbourne, Australia) and MDM were generated from M-CSF-treated cultures (36).

Matrix Degradation Assay—Macrophage matrix degradation was determined as before (8). Briefly, macrophages (3×10^4) were cultured on FITC-coupled gelatin for 24–48 h in the presence of M-CSF (2000 units/ml), plasminogen (500 nM), RgpA-Kgp (5–50 nM), anti-uPA mAb (267 nM), and isotype control mAb (267 nM) as indicated. Cells were processed for F-actin and DAPI staining and visualized by fluorescent microscopy (Zeiss Axioskop 2, at ×40 magnification). Images were captured by a Zeiss AxioCam MRm and quantification of matrix degradation by calculating the area of gelatin degradation per total cell area (ImageJ, version 1.46) (8). Six random fields were analyzed for each group, and the assays were performed in four independent experiments.

Quantitative PCR—Total RNA was extracted using RNeasy kits (Qiagen) and reverse transcribed using SuperScript III (Invitrogen). Quantitative PCR was performed using an ABI PRISM 7900HT sequence detection system (Applied Biosystems, Carlsbad, CA) and TaqMan probe/primer combinations for human and murine uPA, uPAR, and Ubiquitin C (Applied Biosystems) (32). All samples were performed in triplicate, and results are expressed relative to UBC from five independent experiments.

Analysis of Pro-uPA Activation by Western Blot and SDS-PAGE—For Western blotting, human pro-uPA (250 nM) was incubated with plasmin (10 nM) or RgpA-Kgp complex (10 nM) in reaction buffer (0.5 M Tris/HCl, pH 7.4) at 37 °C for up to 60 min. Reactions were terminated by 5× SDS sample buffer and heating to 95 °C for 10 min. Samples were analyzed under reducing conditions by SDS-PAGE (Invitrogen), and uPA was detected with an anti-human uPA mAb (clone U-16) by Western blotting. Alternatively, human pro-uPA (4.5 μM) was incubated with plasmin (50 nM) or RgpA-Kgp complex (50 nM) at 37 °C for 10 min. Reactions were terminated by 5× SDS and heated to 95 °C for 10 min. Samples were analyzed by SDS-PAGE with proteins bands visualized with EzBlue gel staining reagent (Sigma).

Cleavage Site Determination by Sulfo-NHS-acetate Labeling and Tandem Mass Spectrometry—RgpA-Kgp complex (50 nM) was incubated for 10 min with human pro-uPA (4.5 μM) at 37 °C in PBS. Samples were labeled as before (37). Briefly, sam-

ples were precipitated at 4 °C for 30 min and air-dried at room temperature. The pellets were resuspended in 0.2% SDS and 100 mM $NaHCO_3$, pH 8.5, and sonicated for 20 min, labeled with 10 mM sulfo-NHS-acetate for 60 min, and quenched with 10 mM of Tris/HCl, pH 8.0. Denatured samples were run on SDS-PAGE with trypsin in-gel digestion performed after reduction with DTT and alkylation with iodoacetamide (37). Tryptic digests were analyzed by LC-MS/MS using a Dionex Ultimate 3000 system (Thermo Scientific) coupled to an HCTultra ion trap mass spectrometer (37). Proteins were identified by MS/MS Ion Search using Mascot v 2.2 (Matrix Science) against the SwissProt database (June 2014) with taxonomy restricted to *Homo sapiens*. Search parameters were: enzyme = trypsin (with results of semi-trypsin search also checked); missed cleavages = 3; fixed modifications = carbamidomethyl (Cys); optional modifications = acetyl (Lys), acetyl (N terminus), and oxidation (Met); MS tolerance = 1.5 Da; and MS/MS tolerance = 0.5 Da.

Chromogenic Assays—For pro-uPA activation: 0.6 mM chromogenic uPA substrate (S2444), 50 nM human pro-uPA, 10 nM human plasmin, 10 nM RgpA-Kgp complex were mixed in assay buffer (0.5 M Tris/HCl, pH 7.4, with 0.1% (v/v) Tween 20) in the presence or absence of human PAI-1 (100 nM) or α2-antiplasmin (100 nM) as indicated. The dose-dependent activation of human pro-uPA (50 nM) by plasmin (25 to 0.1 nM) and RgpA-Kgp complex (25 to 0.1 nM) was determined at 60 min. Reactions were performed at 37 °C with absorbance measured at 405 nm for 90 min in a Bio-Rad 680 reader. For plasminogen activation: 0.5 mM chromogenic plasmin substrate (S2251), 250 nM human plasminogen, 50 nM human uPA, and 50 nM RgpA-Kgp complex were mixed in assay buffer (as above). Substrate conversion over 180 min was measured by absorbance at 405 nm. The dose-dependent activation of plasminogen (250 nM) by uPA (125 nM to 0.5 nM) and RgpA-Kgp complex (125 to 0.5 nM) was determined at 120 min.

P. gingivalis-induced Periodontitis Model—The murine periodontitis model was previously described (31). Briefly, 12 mice (wild-type and $uPA^{-/-}$ C57BL/6 mice) per group were treated with kanamycin (Sigma) at 1 mg/ml for 7 days followed by a 3-day antibiotic-free period. Oral inoculation on days 0 and 20 with each regime consisting of four doses of *P. gingivalis* W50 (1.0×10^{10} viable *P. gingivalis* W50 cells suspended in 2% (w/v) carboxymethylcellulose vehicle (Sigma)), given 2 days apart. Alveolar bone resorption and subgingival *P. gingivalis* colonization were determined as before (31).

Statistical Analysis—Statistical comparisons between groups were performed using unpaired Student's *t* test (GraphPad Prism 4 software). *p* values ≤0.05 indicate significance. The data were plotted using GraphPad Prism 4.03 software. The data for alveolar bone resorption (mm2) were analyzed using one-way analysis of variance, with a Dunnett's T post hoc test.

Results

RgpA-Kgp Complex Potentiates Mouse Macrophage Matrix Degradation in a uPA-dependent Manner—Oral inoculation of $uPA^{-/-}$ mice with *P. gingivalis* failed to induce significant alveolar bone loss ($p < 0.001$; Fig. 1*A*) in contrast to wild-type mice, which developed significant bone loss relative to uninoculated mice. Also $uPA^{-/-}$ mice had lower levels of *P. gingivalis* in the subgingival plaque compared with wild-type mice (data not shown), suggesting that uPA is necessary for the emergence of the pathogen (29). We have previously demonstrated that macrophage uPA conversion of plasminogen to active plasmin plays a major role in its ability to degrade matrix (8) and that depletion of macrophages protects mice from *P. gingivalis*-induced PD (31). Given that PD is characterized by the irreversible destruction of periodontal tissue (17), we speculated that the major virulence factor from *P. gingivalis*, the RgpA-Kgp complex, might enhance the ability of macrophages to degrade matrix. To address this hypothesis and to begin to explore potential mechanistic explanations for the protection of $uPA^{-/-}$ mice in experimental PD, murine BMM were seeded on FITC-gelatin-coated coverslips in the presence of plasminogen and/or RgpA-Kgp complex and matrix degradation quantified by fluorescent microscopy.

As shown in Fig. 1*B*, BMM had a low capacity to degrade matrix, which was significantly increased by the addition of plasminogen ($p < 0.05$; Fig. 1*C* for quantification). Strikingly, this plasminogen-induced matrix breakdown could be further enhanced by the addition of the RgpA-Kgp complex with a 4–5-fold increase in FITC-gelatin degradation by macrophages co-treated with RgpA-Kgp complex and plasminogen *versus* those treated with plasminogen alone ($p < 0.05$; Fig. 1, *B* and *C*). A dose response was observed where increasing concentrations of RgpA-Kgp complex enhanced BMM FITC-gelatin degradation ($p < 0.05$; Fig. 2, *A* and *B* for quantification). Treatment of BMM with the RgpA-Kgp complex in the absence of plasminogen did not enhance matrix breakdown (Fig. 1, *B* and *C*). It was also observed that in the absence of macrophages, the RgpA-Kgp complex either in the absence or presence of plasminogen did not degrade the FITC-gelatin matrix (data not shown). These findings show that the gingipain itself did not degrade the matrix and that macrophages are required for matrix degradation. Importantly, we found that treatment of BMM with the anti-uPA mAb, mU1, which blocks the function of murine uPA *in vivo* (33), abrogated the ability of the RgpA-Kgp complex and plasminogen combination to potentiate macrophage-mediated matrix degradation ($p < 0.05$; Fig. 1, *B* and *C*). One possible mechanism for the enhancement of uPA-dependent matrix breakdown is increased uPA and uPAR gene expression in macrophages treated with RgpA-Kgp complex. However, when BMM were treated with the RgpA-Kgp complex, we did not observe any significant changes in uPA or uPAR gene expression relative to untreated cells (Fig. 1*D*). These data demonstrate that *P. gingivalis*-derived RgpA-Kgp complex potentiates macrophage matrix breakdown in a uPA-dependent manner, which could not be explained by the ability of the complex to modulate uPA and uPAR expression.

RgpA-Kgp Complex Potentiates Human Macrophage Matrix Degradation in a uPA-dependent Manner—We next addressed whether RgpA-Kgp complex could potentiate human MDM matrix degradation. Similar to BMM (Fig. 1*B*), MDM matrix degradation was significantly enhanced by the addition of plasminogen ($p < 0.05$; Fig. 3, *A* and *B* for quantification) (8). Again, we found a striking increase in matrix breakdown (an approximately 3–4-fold increase in FITC-gelatin degradation) by

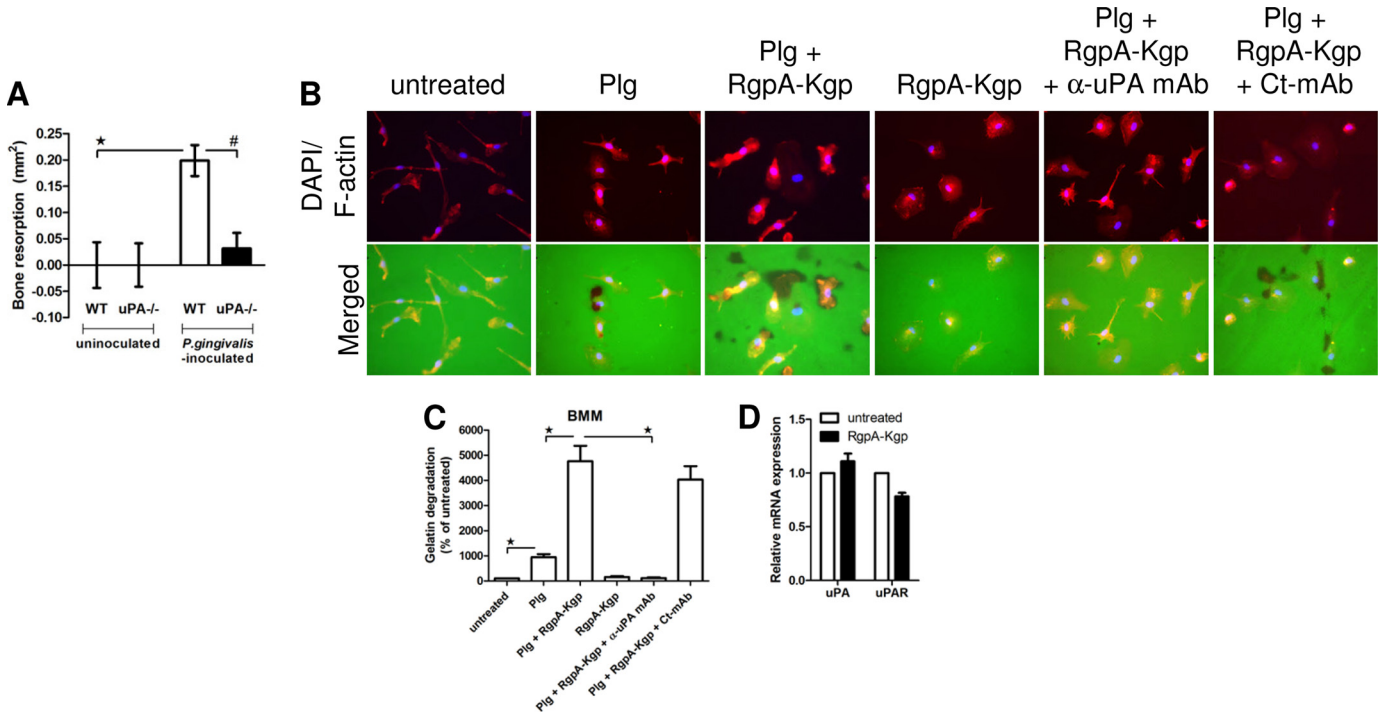

FIGURE 1. **uPA$^{-/-}$ mice are protected from *P. gingivalis*-induced bone loss, and the RgpA-Kgp complex potentiates murine macrophage matrix degradation in a uPA-dependent manner.** *A*, wild-type and *uPA*$^{-/-}$ mice were orally inoculated with *P. gingivalis* or buffer alone (uninoculated group). Alveolar bone resorption was determined, and the data are expressed as the mean ± S.D. in mm^2. The data were analyzed using a one-way analysis of variance and Dunnett's T3 post hoc test ($n = 12$). ⋆, $p \leq 0.001$; #, $p \leq 0.001$. *B*, BMM (3×10^4 cells/well) were placed on FITC-gelatin-coated coverslips (48 h), either untreated or in the presence of plasminogen (*Plg*) (500 nM), the RgpA-Kgp complex (5 nM), anti-mouse uPA mAb mU1 (267 nM), and control mAb as indicated. Cells were stained with TRITC-phalloidin (*top panel*, *red*) and DAPI (*top panel*, *blue*), and FITC-gelatin degradation (*bottom panel*, merged) was visualized in areas devoid of FITC staining by fluorescent microscopy at ×40 magnification. Shown are data from a representative of four independent experiments. *C*, quantification of FITC-gelatin degradation by BMM. The area of gelatin degradation per total cell area was determined and expressed as a percentage ± S.D. relative to untreated cells ($n = 4$). ⋆$p \leq 0.05$ (Student's *t* test) (8). *D*, BMM were stimulated with the RgpA-Kgp complex (20 nM for 24 h), and the relative gene expression of murine uPA and uPAR was measured by qPCR. The data were normalized to UBC reference gene and expressed relative to untreated cells ± S.D. ($n = 5$).

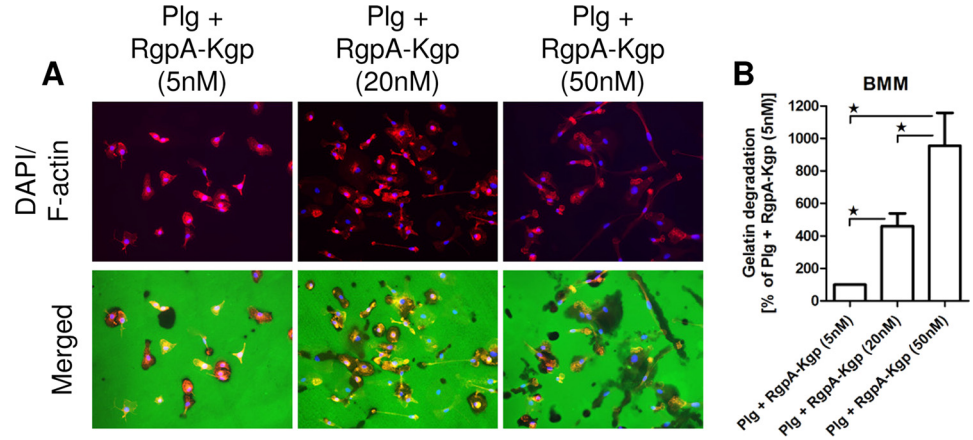

FIGURE 2. **Dose-dependent increase in mouse macrophage matrix degradation by RgpA-Kgp complex.** *A*, BMM (3×10^4 cells/well) were placed on FITC-gelatin-coated coverslips (48 h), in the presence of plasminogen (*Plg*) (500 nM) and increasing concentrations of RgpA-Kgp complex (5, 20, or 50 nM). Cells were stained with TRITC-phalloidin (*top panel*, *red*) and DAPI (*top panel*, *blue*), and FITC-gelatin degradation (*bottom panel*, merged) was visualized in areas devoid of FITC staining by fluorescent microscopy at ×20 magnification. Shown are data from a representative of three independent experiments. *B*, quantification of FITC-gelatin degradation by BMM. The area of gelatin degradation per total cell area was determined and expressed as a percentage ± S.D. relative to cells treated with Plg + RgpA-Kgp (5 nM). ⋆, $p \leq 0.05$ (Student's *t* test, $n = 3$).

MDM co-treated with the RgpA-Kgp complex and plasminogen *versus* those treated with plasminogen alone. Neutralizing anti-human uPA mAb (U-16) potently blocked MDM matrix degradation induced by plasminogen and RgpA-Kgp complex ($p < 0.05$; Fig. 3, *A* and *B*). In MDM, as in BMM (Fig. 1*D*), the RgpA-Kgp complex did not regulate uPA or uPAR gene expression (Fig. 3*C*), further substantiating that the RgpA-Kgp complex potentiation of macrophage degradation is not caused by increased gene expression of uPA or its receptor.

RgpA-Kgp Complex Cleaves Latent Pro-uPA—Given that pro-uPA requires proteolytic cleavage at a lysine consensus site to become active (11), we hypothesized that the intrinsic lysine activity of the Kgp gingipain may allow it to cleave and activate pro-uPA, potentially explaining the ability of the RgpA-Kgp

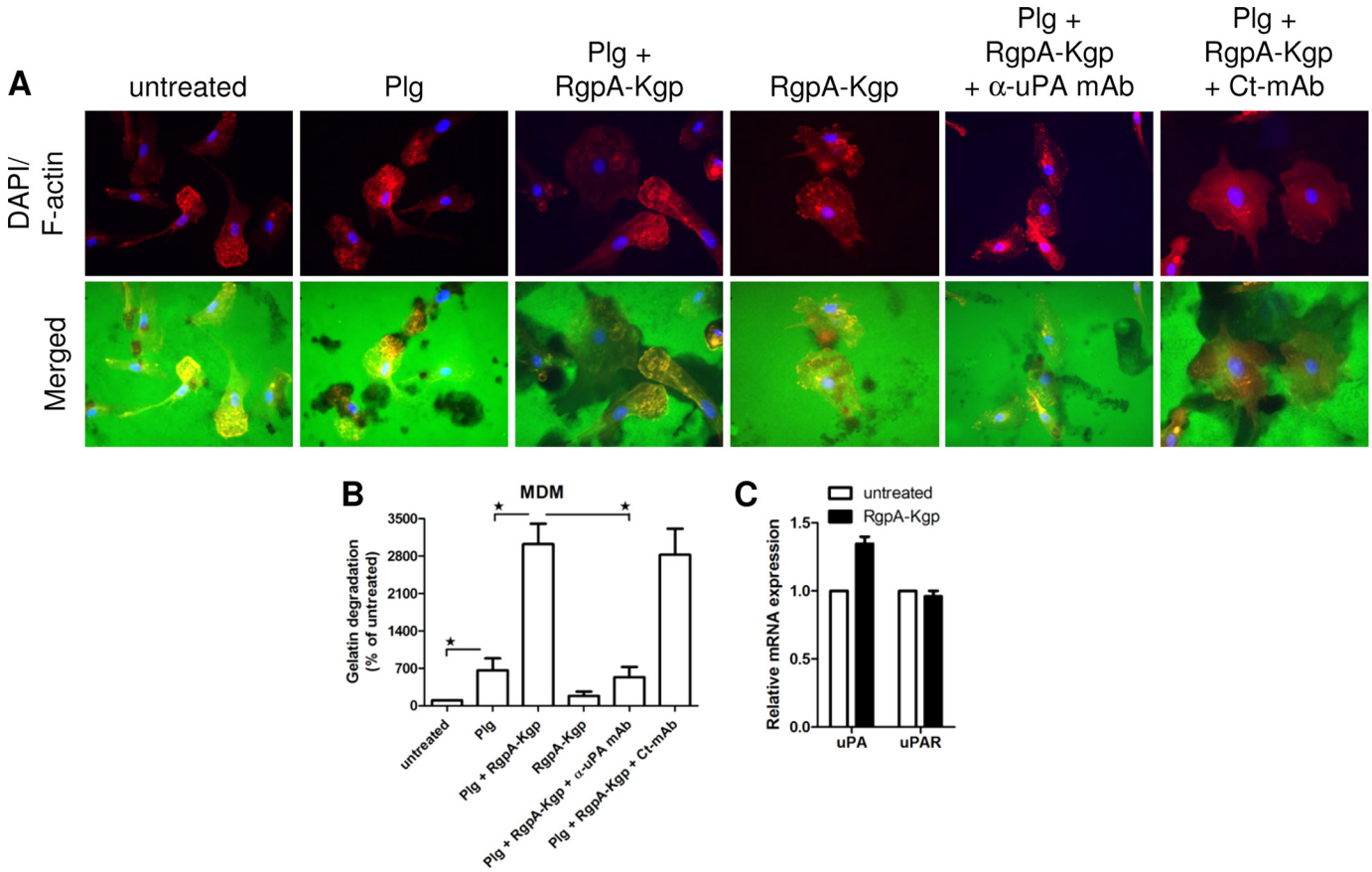

FIGURE 3. **The RgpA-Kgp complex potentiates human macrophage matrix degradation in a uPA-dependent manner.** *A*, MDM (3×10^4 cells/well) were placed on FITC-gelatin-coated coverslips (24 h), either untreated or in the presence of plasminogen (*Plg*) (500 nM), RgpA-Kgp complex (5 nM), anti-human uPA mAb U-16 (267 nM), and control mAb as indicated. Cells were stained with TRITC-Phalloidin (*top panel*, *red*), DAPI (*top panel*, *blue*), and FITC-gelatin degradation (*bottom panel*, merged) was visualized in areas devoid of FITC staining by fluorescent microscopy at ×40 magnification. Shown are data from a representative of four independent experiments. *B*, quantification of FITC-gelatin degradation by MDM. The area of gelatin degradation per total cell area was determined and expressed as a percentage ± S.D. relative to untreated cells ($n = 4$). ⋆, $p \leq 0.05$ (Student's *t* test). *C*, MDM were stimulated with RgpA-Kgp complex (20 nM for 24 h), and the relative gene expression of human uPA and uPAR was measured by qPCR. The data were normalized to that of the UBC reference gene and expressed relative to untreated cells ± S.D. ($n = 5$).

complex to enhance uPA-dependent macrophage-mediated matrix degradation (Figs. 1*B* and 3*A*). To test this, cleavage of human pro-uPA by the RgpA-Kgp complex was compared with cleavage by the major physiologic regulator of uPA, plasmin. Plasmin cleavage of single-chain pro-uPA can occur at two major sites (12): proteolysis at the primary site (Lys^{158}-Ile^{159}) generates the A-chain (20 kDa) and B-chain (30 kDa), whereas processing at the secondary site (Lys^{135}-Lys^{136}) yields LMW-uPA (33 kDa) and the N-terminal fragment (18 kDa).

Accordingly, when human pro-uPA was incubated with plasmin for 10 min and the resulting fragments were separated by SDS-PAGE, four major fragments were generated corresponding to LMW-uPA (*band I*, 33 kDa), B-chain (*band II*, 30 kDa), A-chain (*band III*, 20 kDa), and N-terminal fragment (*band IV*, 18 kDa) (Fig. 4*A*, *left lane*). Incubation of RgpA-Kgp complex with pro-uPA for 10 min yielded identically sized fragments at 33 kDa (*band I*) and 30 kDa (*band II*), consistent with the generation of LMW-uPA and B-chain, respectively (Fig. 4*A*, *lane 2*). Identical fragments at 20 kDa (Fig. 4*A*, *band III*) and 18 kDa (Fig. 4*A*, *band IV*) were also generated by the RgpA-Kgp complex but were much weaker than those generated by plasmin. RgpA-Kgp complex cleavage of pro-uPA also generated a smaller band of ~15 kDa (Fig. 4*A*, *band V*) that was not generated by plasmin.

We next analyzed the kinetics of pro-uPA cleavage by RgpA-Kgp complex *versus* plasmin by Western blot using an anti-uPA mAb targeting the protease domain. Plasmin rapidly and completely cleaved single-chain pro-uPA (labeled P, 55 kDa) to generate a protease domain-containing band even after 1 min (Fig. 4*B*). This is consistent with the complete cleavage of pro-uPA by plasmin seen by SDS-PAGE in Fig. 4*A*. In comparison, RgpA-Kgp cleavage of pro-uPA was slower with a protease domain-containing band not detected until 30 min (Fig. 4*B*); also the cleavage of single-chain pro-uPA was incomplete, with intact pro-uPA still present at 60 min. The bands generated by RgpA-Kgp complex *versus* plasmin cleavage of pro-uPA were identical in size (~30 kDa) and were similar in size to the protease domain-containing LMW-uPA (*band I*, ~33 kDa) and B-chain (*band II*, ~30 kDa) observed in Fig. 4*A*; however, these two distinct bands could not be clearly identified by Western blot. Together, these data show that the RgpA-Kgp complex cleavage of pro-uPA generates fragments similar to those generated by its physiologic activator, plasmin, but with slower kinetics.

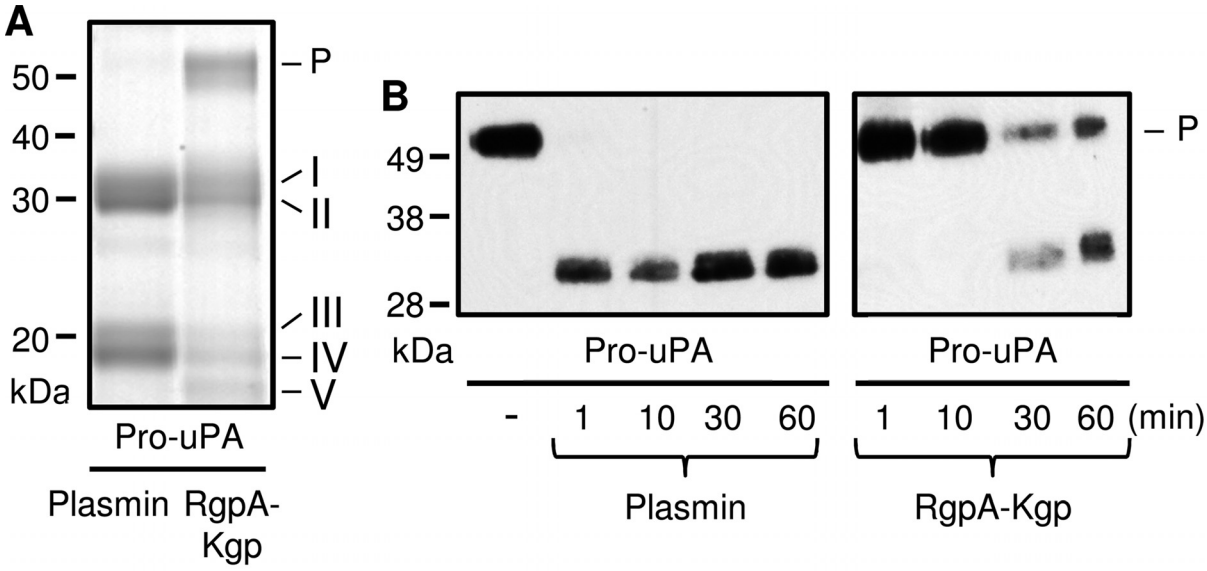

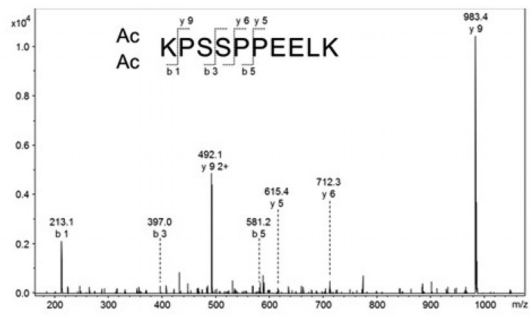

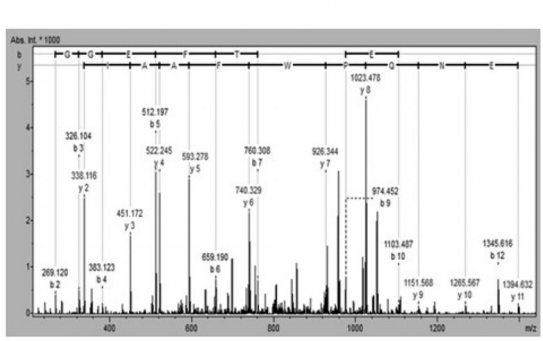

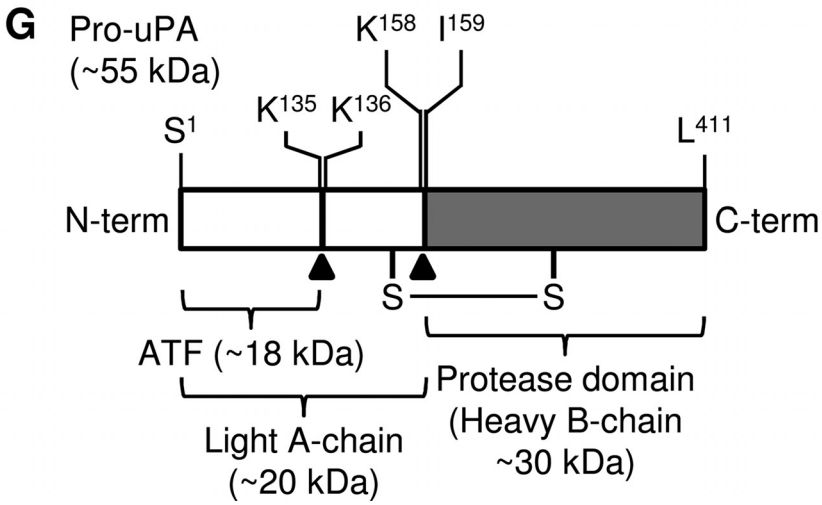

RgpA-Kgp Complex Cleaves Pro-uPA at the Major Consensus Sites—To confirm that the RgpA-Kgp complex cleaves human pro-uPA at the same sites as plasmin (Lys^{158}-Ile^{159} and Lys^{135}-Lys^{136}) (11, 13), the RgpA-Kgp-cleaved pro-uPA fragments (Fig. 4*A*, *lane* 2) were labeled and identified by mass spectrometry. Specifically, the N terminus of each pro-uPA fragment was acetylated with sulfo-NHS-acetate, which acetylates free primary amines on the side chain of Lys residues and the N terminus of polypeptides. The labeled fragments were then separated by SDS-PAGE (Fig. 4*A*, *lane 2*), digested with trypsin, and identified by LC-MS/MS.

Peptides identified from the 33-kDa band (Fig. 4*A*, *band I*) indicated that this fragment included amino acids from Lys^{136} to the C terminus of the protein at Leu^{411}, conforming to the sequence of LMW-uPA (Fig. 4*C*, peptides identified are shown in bold and underlined). Importantly, the most N-terminal peptide identified (^{136}KPSSPPEELK^{145}) (Fig. 4*C*, *arrowhead*) was doubly acetylated at the N-terminal K residue, indicating that both the Lys side chain and the N terminus were acetylated. The N-terminal acetylation shows that this amino group was free at the time of labeling thereby, confirming that the RgpA-Kgp complex cleaved pro-uPA at the consensus site Lys^{135}-Lys^{136} (13). The MS/MS data for this peptide (^{136}KPSSPPEELK^{145}) did not give a significant Mascot score because of the highly favored fragmentation of the three Xaa-Pro bonds in the sequence (38); however, the fragmentation pattern was consistent with the sequence (Fig. 4*D*).

Peptides identified from the 30-kDa band (Fig. 4*A*, *band II*) included amino acids from Ile^{159} to the C terminus of the protein at Leu^{411}, conforming to the sequence of the B-chain of uPA (Fig. 4*E*, peptides identified are shown in bold and underlined). The N-terminal peptide (^{159}IIG . . . IYR^{178}) was acetylated at the N terminus and gave a rich fragmentation pattern yielding a high Mascot score of 94 (Fig. 4*F*), confirming that the RgpA-Kgp complex, like plasmin, cleaves the Lys^{158}-Ile^{159} bond of pro-uPA (Fig. 4*F*, *arrowhead*) (11). The analysis of the 20- and 18-kDa bands (Fig. 4*A*, *bands III* and *IV*) proved inconclusive and did not allow us to identify these bands as the A-chain (*band III*) or the N-terminal fragment (*band IV*) of uPA, respectively. However, these data confirm for the first time that the *P. gingivalis*-derived RgpA-Kgp complex cleaves pro-uPA at the common activation sites (Lys^{158}-Ile^{159} and Lys^{135}-Lys^{136}) (11, 13) to generate the protease domain-containing LMW-uPA and B-chain (Fig. 4*G*).

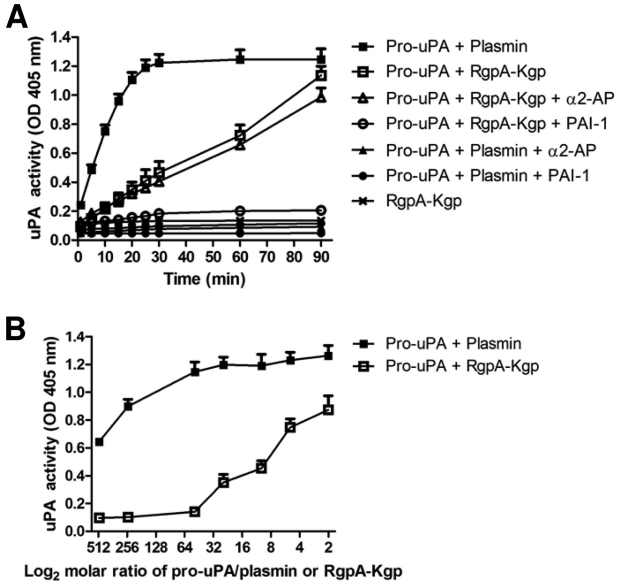

FIGURE 5. **The RgpA-Kgp complex activates pro-uPA to form uPA.** *A*, human pro-uPA activation by plasmin and RgpA-Kgp complex were compared in a kinetic chromogenic assay. Pro-uPA (50 nM) was incubated with plasmin (10 nM) or the RgpA-Kgp complex (10 nM) in the presence of the inhibitors α2-antiplasmin (*α2-AP*, 100 nM) or PAI-1 (100 nM). The uPA-specific substrate (0.6 mM; S2444) and absorbance was monitored for 90 min at 37 °C at 405 nm. *B*, comparison of the dose-dependent activation of pro-uPA (50 nM) by plasmin and the RgpA-Kgp complex (25 to 0.1 nM). The molar ratios measured were 500, 250, 50, 25, 10, 5, and 2 of pro-uPA to 1 of plasmin or RgpA-Kgp. The data are plotted on a $\log_2$ scale. Absorbance at 405 nm was measured after 60 min at 37 °C ($n = 5$, $\pm$ S.D.).

RgpA-Kgp Complex Activates Pro-uPA—Having found that the RgpA-Kgp complex cleaves human pro-uPA at the major consensus sites, we next assessed the enzymatic function of the pro-uPA cleavage products generated by the RgpA-Kgp complex using an enzymatic assay. Human pro-uPA was incubated with RgpA-Kgp complex or plasmin in the presence of the uPA-specific chromogenic substrate (S2444) (33), and the resultant uPA activity measured over 90 min (Fig. 5*A*). Plasmin rapidly induced uPA activity with maximum activation reached at 25–30 min. In comparison, the RgpA-Kgp complex initially led to a slower rate of uPA activity, which is consistent with the kinetics for the generation, by the gingipain complex, of the protease domain-containing band by Western blot (Fig. 4*B*). Ultimately, uPA activity induced by the RgpA-Kgp complex, reached a comparable peak to that induced by plasmin at 90 min (Fig. 5*A*). Importantly, the RgpA-Kgp complex did not

FIGURE 4. **The RgpA-Kgp complex cleaves pro-uPA at the major consensus sites.** *A*, pro-uPA (4.5 μM) was incubated with plasmin (50 nM) or the RgpA-Kgp complex (50 nM) for 10 min, reaction mixtures were separated by SDS-PAGE (12%) under reducing conditions, and protein bands were stained with Coomassie Brilliant Blue. Samples were labeled prior to separation by SDS-PAGE as before (see "Experimental Procedures") (37). Indicated are intact pro-uPA (labeled P, 55 kDa) and the major fragments produced: *band I* (33 kDa), *band II* (30 kDa), *band III* (20 kDa), *band IV* (18 kDa), and *band V* (15 kDa). *B*, time-dependent cleavage of pro-uPA (250 nM) by plasmin (10 nM) or the RgpA-Kgp complex (10 nM) measured at 1, 10, 30, and 60 min by Western blot. Protein bands were detected with anti-uPA mAb specific for the protease domain of uPA. Indicated is the intact single-chain pro-uPA (labeled P, 55 kDa). Western blots were performed under reducing conditions. *C*, peptides from *band I* included amino acids from Lys^{136} to Leu^{411} of the primary human uPA sequence conforming to the sequence of LMW-uPA. The N-terminal peptide (^{136}KPS . . . ELK^{145}) was doubly acetylated, confirming that the RgpA-Kgp complex cleaved at the consensus Lys^{135}-Lys^{136} site (indicated with *arrowhead*). *D*, MS/MS spectra of the most N-terminal peptide detected for *band I*. Although the Mascot score was low for this peptide (because of the prolines in the sequence; see main text), the fragmentation pattern was consistent with the sequence and indicated the presence of two acetyl groups at the N-terminal lysine residue. *E*, peptides from *band II* included amino acids from Ile^{159} to Leu^{411}, conforming to the sequence of the uPA B-chain. The N-terminal peptide (^{159}IIG . . . IYR^{178}) was acetylated, confirming that the RgpA-Kgp complex cleaved at the consensus Lys^{158}-Ile^{159} site (indicated with *arrowhead*). *F*, MS/MS spectra of the most N-terminal peptide detected for *band II*. This rich spectrum matched to the sequence Ac-IIGGEFTTIENQPWFAAIYR with a high Mascot score of 94. *G*, schematic showing the domain structure of human pro-uPA and the major cleavage sites of plasmin and RgpA-Kgp complex (indicated with *arrowheads* at Lys^{135}-Lys^{136} and Lys^{158}-Ile^{159}). The A- and B-chains of uPA are held together by a single interchain disulfide bond (represented by S-S).

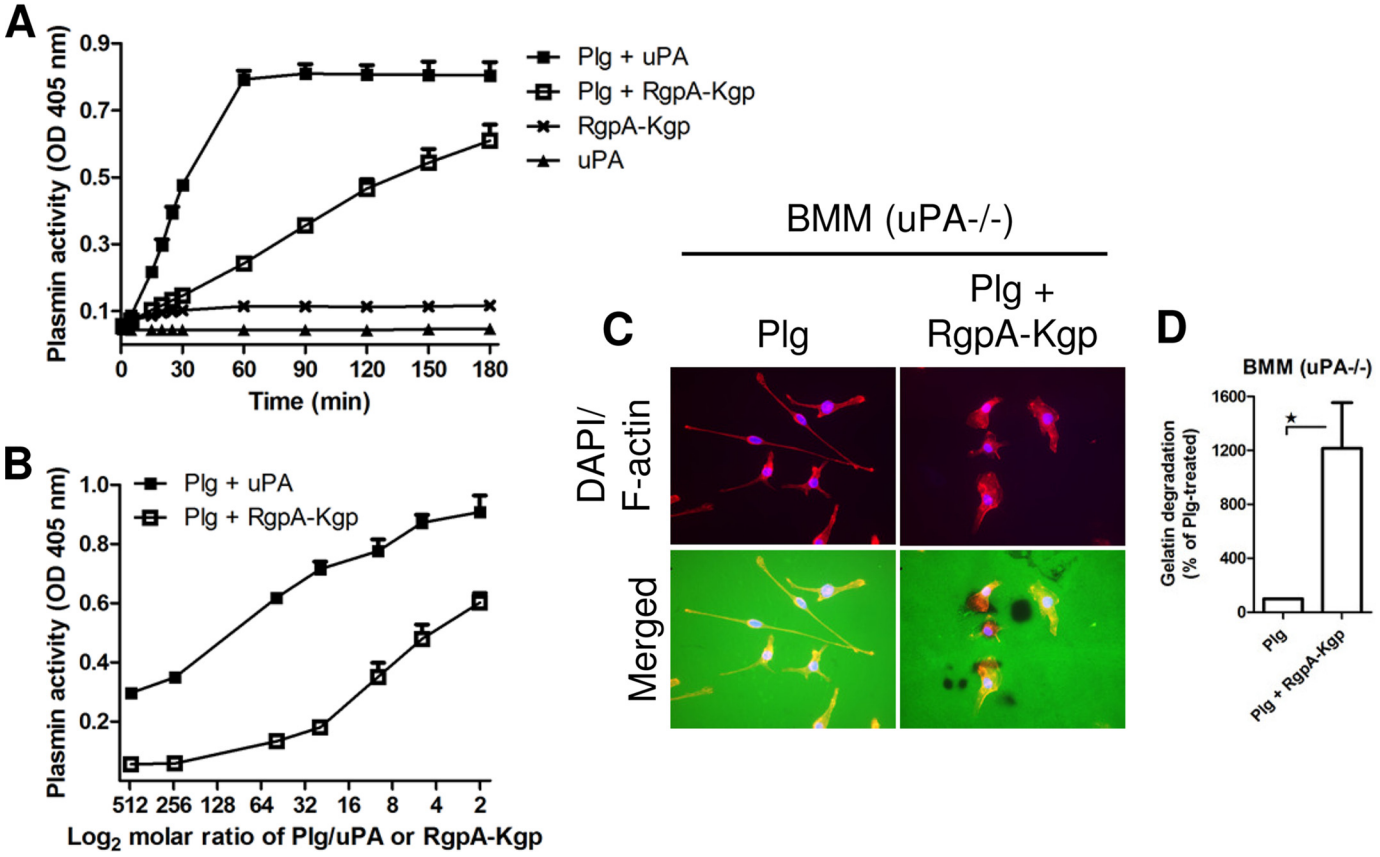

FIGURE 6. **The RgpA-Kgp complex activates plasminogen to form plasmin.** *A*, plasminogen activation by uPA and RgpA-Kgp complex were compared in a kinetic chromogenic assay. Plasminogen (250 nM) was incubated with uPA (50 nM) or RgpA-Kgp complex (50 nM) in the presence of the plasmin-specific substrate (0.5 mM; S2251), and absorbance was monitored at 405 nm for 180 min at 37 °C. *B*, comparison of the dose-dependent activation of plasminogen (250 nM) by uPA and the RgpA-Kgp complex (125 nM to 0.5 nM). The molar ratios measured were 500, 250, 50, 25, 10, 5, and 2 of plasminogen to 1 of uPA or RgpA-Kgp. The data are plotted on a $\log_2$ scale. Absorbance at 405 nm was measured after 120 min at 37 °C ($n = 5$, ± S.D.). *C*, uPA$^{-/-}$ BMM (3×10^4 cells/well) were placed on FITC-gelatin-coated coverslips (48 h), in the presence of Plg (500 nM) or in the presence of Plg + RgpA-Kgp complex (5 nM). Cells were stained with TRITC-Phalloidin (*top panel*, *red*) or DAPI (*top panel*, *blue*), and FITC-gelatin degradation (*bottom panel*, merged) was visualized in areas devoid of FITC staining by fluorescent microscopy at ×40 magnification. Shown are data from a representative of three independent experiments. *D*, the area of gelatin degradation per total cell area was determined and expressed as a percentage ± S.D. relative to cells treated with plasminogen alone ($n = 3$). ⋆, $p \leq 0.05$ (Student's *t* test).

directly cleave the uPA-specific chromogenic substrate (Fig. 5*A*). The specific plasmin inhibitor, α2-antiplasmin, blocked plasmin-induced activation of pro-uPA, whereas the uPA inhibitor, PAI-1, completely blocked uPA activity (generated by plasmin activation of pro-uPA) (Fig. 5*A*). In comparison, α2-antiplasmin had no effect on the ability of the RgpA-Kgp complex to activate pro-uPA, whereas PAI-1 blocked the uPA activity generated by RgpA-Kgp complex activation of pro-uPA (Fig. 5*A*).

When pro-uPA was incubated with different concentrations of the RgpA-Kgp complex or plasmin and uPA activity measured at 60 min (Fig. 5*B*), we found that low concentrations (*i.e.* a molar ratio of 1:500 to 1:50 of RgpA-Kgp to pro-uPA) of the RgpA-Kgp complex was inefficient at activating pro-uPA compared with plasmin. For example, at a molar ratio of 1:50, the RgpA-Kgp complex induced ~15% of the plasmin-induced uPA activity. At higher concentrations (*i.e.* a molar ratio of 1:25 to 1:2 of RgpA-Kgp to pro-uPA), the RgpA-Kgp complex was much more efficient at activating pro-uPA with ~70% of the plasmin-induced uPA activity at a molar ratio of 1:2 (Fig. 5*B*). These results demonstrate that cleavage of pro-uPA by the RgpA-Kgp complex produces enzymatically active uPA, which is consistent with its cleavage at the major consensus site within pro-uPA (Fig. 4*G*).

RgpA-Kgp Complex Cleaves and Activates Plasminogen—The major substrate of uPA is plasminogen, which is a zymogen that requires proteolytic cleavage to form the active serine protease, plasmin. This cleavage occurs at the Arg^{561}-Val^{562} peptide bond to yield the active two-chain protein, which is comprised of a heavy chain (~63 kDa) and a protease domain-containing light chain (~25 kDa) that are linked by a disulfide bond (11). Given the intrinsic arginine activity of the RgpA gingipain, we next sought to determine whether the RgpA-Kgp complex could also cleave and activate plasminogen.

To begin to address this question, we used an enzymatic assay in which plasminogen is incubated with uPA or the RgpA-Kgp complex in the presence of the plasmin-specific chromogenic substrate (S2251) (33), and the resulting plasmin activity is then measured over 180 min. Fig. 6*A* shows that the activation of plasminogen by uPA reached maximum levels at ~60 min. The RgpA-Kgp complex induced plasminogen activation but with delayed kinetics relative to uPA (Fig. 6*A*). Early on (0–30 min), the RgpA-Kgp complex only weakly induced plasmin activity, but at 180 min the plasmin activity induced by the

RgpA-Kgp complex was ~75% of the uPA-induced plasmin activity. Neither the RgpA-Kgp complex nor uPA directly cleaved the plasmin-specific chromogenic substrate (Fig. 6*A*).

The abilities of uPA and RgpA-Kgp complex to activate plasminogen were further compared by incubating plasminogen with different concentrations of uPA or the RgpA-Kgp complex and measuring plasmin activity at 120 min (Fig. 6*B*). At low concentrations (*i.e.* a molar ratio of 1:500 to 1:250 of RgpA-Kgp to plasminogen), the RgpA-Kgp complex was inefficient at activating plasminogen compared with uPA. For example, at a molar ratio of 1:250, the RgpA-Kgp complex induced ~17% of the uPA-induced plasmin activity (Fig. 6*B*). At higher concentrations (*i.e.* a molar ratio of 1:10 to 1:2 of RgpA-Kgp to plasminogen), the RgpA-Kgp complex was much more efficient at activating plasminogen with ~67% of the uPA-induced plasmin activity at a molar ratio of 1:2 (Fig. 6*B*). These findings demonstrate that not only can the RgpA-Kgp complex activate pro-uPA to uPA, but it can also activate plasminogen to plasmin.

We have previously shown that unlike wild-type cells, $uPA^{-/-}$ macrophages do not respond to exogenous plasminogen for increased matrix degradation (8). Given we show that the RgpA-Kgp complex has intrinsic uPA-like activity in being able to activate plasminogen to plasmin, we reasoned that treatment of $uPA^{-/-}$ macrophages with the RgpA-Kgp complex might "restore" their ability to degrade matrix in the presence of plasminogen. To test this, FITC-gelatin matrix degradation by $uPA^{-/-}$ BMM was determined. As before (8), $uPA^{-/-}$ BMM treated with plasminogen did not degrade FITC-gelatin (Fig. 6*C*). However, when they were co-treated with the RgpA-Kgp complex and plasminogen, a significant increase in FITC-gelatin degradation was observed ($p < 0.05$; Fig. 6, *C* and *D*, for quantification). Indeed, the levels of matrix degradation by wild-type *versus* $uPA^{-/-}$ BMM co-treated with RgpA-Kgp complex and plasminogen were similar (compare Figs. 1*B* and 6*C*). These data suggest that in the absence of uPA, the intrinsic arginine activity of the RgpA gingipain can activate plasminogen to plasmin and restore macrophage matrix degradation.

Discussion

PD is characterized by a high rate of matrix turnover that depends on the regulated expression of proteolytic enzymes (39). *P. gingivalis* gingipains are powerful proteolytic enzymes that can degrade host proteins but can also activate host pathways. This unique ability allows *P. gingivalis* to generate nutrients in the form of tissue breakdown products and to subvert the host immune response, leading to periodontal inflammation and dysbiosis (21, 22). uPA has been identified in inflamed periodontal tissue (26) and in the gingival crevicular fluid (27). Our findings here provide evidence of a new host pathway that can be activated by *P. gingivalis* gingipains, namely the uPA/plasminogen pathway. Specifically, we find that the RgpA-Kgp complex has intrinsic plasmin-like and uPA-like enzymatic activities in being able to activate host zymogens, pro-uPA, and plasminogen, respectively. In the case of pro-uPA, the RgpA-Kgp complex cleaved at the major consensus sites (Lys^{158}-Ile^{159} and Lys^{135}-Lys^{136}) (11, 13) to yield enzymatically active uPA. The RgpA-Kgp complex also activated plasminogen, which is present in micromolar concentrations in extracellular fluids (40) to yield active plasmin.

Much of the damage to the periodontal tissue in PD is now recognized to be caused by the destructive host inflammatory response (41). We have shown that macrophages (31) and uPA (29) are important in the *P. gingivalis*-induced PD model. Interestingly, protection of $uPA^{-/-}$ mice in the *P. gingivalis*-induced PD model was associated with reduced numbers of macrophages in the gingival tissue (29), consistent with our data showing a critical role for uPA in promoting macrophage adhesion and motility (8). Indeed, we have speculated (8) that uPA may play an important role in controlling macrophage retention within certain inflammatory lesions, which may help to explain the benefit of its targeting in inflammatory disease (7, 9, 10, 42); our prior data showing a uPA dependence for three systemic arthritis models (9, 10) suggest that elevated uPA activity could be a common feature of PD and rheumatoid arthritis, perhaps helping to explain their association (43). The ability of the RgpA-Kgp complex to amplify the uPA/plasminogen-mediated matrix degradation by macrophages provides a potential mechanism for enhanced matrix turnover in PD. Because macrophages express high levels of uPAR and various receptors for plasminogen (*e.g.* annexin A2 and Plg-R_{KT}) (44, 45), thereby localizing the activation of pro-uPA and plasminogen to the cell surface (4), it is likely that the gingipain complex is acting in close proximity to the cell surface uPAR-uPA complex. Indeed, it is known that Kgp binds vitronectin, a component of the extracellular matrix and a ligand for uPAR (46, 47). A functional consequence of the focal proteolysis mediated by the uPAR-uPA complex is facilitation of cell migration through complex matrices (4, 15). Whether RgpA-Kgp complex activation of the macrophage uPA/plasminogen pathway regulates cell motility is currently unknown. Its effects on other cell types that express uPA (*e.g.* neutrophils and fibroblasts) (4) are also unknown.

Activation of pro-uPA (to uPA) by plasmin and plasminogen (to plasmin) by uPA occur at lysine and arginine residues, respectively (11, 12). Therefore, it would not be unreasonable to propose that pro-uPA is a substrate for lysine-specific Kgp, whereas plasminogen is a substrate for arginine-specific RgpA. The dual induction of uPA-like and plasmin-like activity by the RgpA-Kgp complex was observed in the context of macrophage matrix degradation. In this system, the intrinsic plasmin-like enzymatic activity (*i.e.* activation of pro-uPA to uPA) of the gingipain complex was evidenced by the potent blockade of matrix degradation by anti-uPA mAbs. In turn, the intrinsic uPA-like enzymatic activity (*i.e.* activation of plasminogen to plasmin) of the complex was evidenced by its ability to restore the plasminogen-mediated matrix degradation by $uPA^{-/-}$ macrophages.

Given this dual induction of uPA and plasmin activity by the gingipain complex, it was expected that uPA blockade (via anti-uPA mAbs) would only partially block macrophage matrix degradation in the presence of plasminogen. However, we were surprised to find an almost complete abrogation of macrophage matrix degradation, when cells were treated with a combination of RgpA-Kgp complex and plasminogen in the presence of the blocking uPA mAbs. The activation of pro-uPA and plas-

minogen are greatly enhanced when both are bound to the cell surface (15, 48). On monocytes-macrophages, the plasminogen receptors Plg-R_{KT} (45, 49) and annexin A2 (50) are co-localized with uPAR (and presumably uPA), with this proximity being central to the reciprocal cell surface activation of uPA and plasmin (45). For the RgpA-Kgp complex to activate pro-uPA to uPA and/or plasminogen to plasmin, it would presumably have to be in very close proximity to the cell-surface uPAR-uPA and plasminogen "complex." It is possible that the neutralizing anti-uPA mAbs (mU1 and U-16), which block the interaction with plasminogen at the active site by steric hindrance (33, 51), may also sterically hinder the large (~250 kDa) gingipain complex from the plasminogen active site. This is currently under investigation because it may explain the nearly complete abrogation of macrophage matrix degradation by anti-uPA mAbs when cells were co-treated with RgpA-Kgp complex and plasminogen.

Cleavage of either pro-uPA or plasminogen by the RgpA-Kgp complex leads ultimately to the generation of the broad spectrum serine protease, plasmin: pro-uPA is most likely to be cellular-derived, whereas plasminogen would be readily available because it circulates at very high levels (14). Plasmin can directly activate components of the complement cascade, such as C3 and C5 (52), and we have shown that uPA is upstream of C5a activation in peritonitis model and is required for optimal C5a generation (10). Activation of the complement cascade has been invoked as a key aspect of the role of *P. gingivalis* as a keystone pathogen (20). Similar to the findings in the $C5aR^{-/-}$ mice, which are resistant to *P. gingivalis* colonization and are thus protected from alveolar bone loss (53), we recently found that *P. gingivalis* poorly colonized the subgingival plaque in $uPA^{-/-}$ mice compared with wild-type mice (29). This likely explains the protection of $uPA^{-/-}$ mice from *P. gingivalis*-induced alveolar bone loss but also suggests that the pathogen depends on uPA to colonize the host and drive inflammation. More specifically, it may suggest the involvement of Kgp-mediated activation of pro-uPA to uPA in *P. gingivalis* colonization. In this context, we have found that of the three proteinases, Kgp is the major contributor to *P. gingivalis* virulence in the murine PD model used here (54). Apart from activating the extracellular uPA proteolytic cascade, the generation of uPA at the cell surface by the gingipain complex may also promote uPA-uPAR signaling, which is independent of uPA proteolytic activity (55), and can regulate cell adhesion, survival and motility (4) (Fig. 7). Interestingly, in the context of our observation that $uPA^{-/-}$ mice were protected from *P. gingivalis*-induced alveolar bone loss (29), a recent study found that uPA-uPAR signaling promoted osteoclastogenesis (56). Whether RgpA-Kgp complex activation of the host uPA/plasminogen pathway occurs in PD as discussed above (Fig. 7) and whether this pathway is linked to the complement-driven dysbiosis and inflammation involved in PD progression are unknown.

Similar to its ability to activate the complement cascade (21), the activation of pro-uPA and plasminogen would likely benefit the pathogen in several important ways. *P. gingivalis* survival and growth is dependent on the peptides that are released during tissue degradation (18). The ability to activate the destructive host uPA/plasminogen pathway leading to heightened

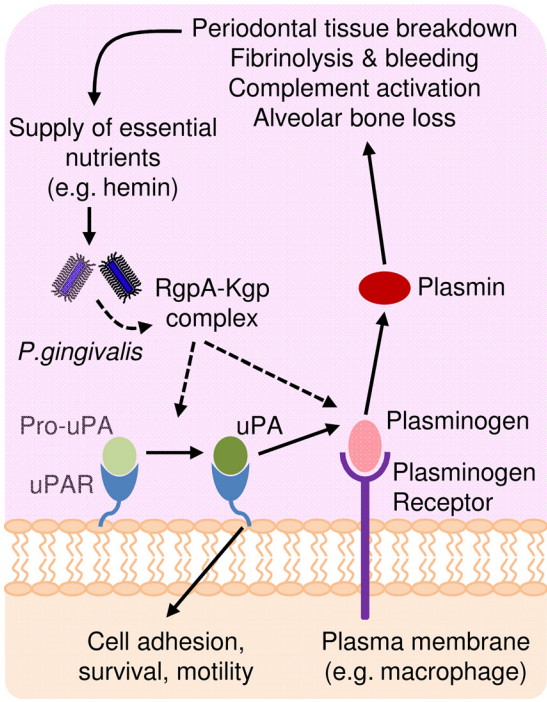

FIGURE 7. **Model of *P. gingivalis* activation of the destructive uPA/plasminogen proteolytic cascade.** *P. gingivalis*-derived RgpA-Kgp complex activation of the uPA/plasminogen pathway (via cleavage and activation of the zymogens, pro-uPA and plasminogen, respectively) initiates a downstream proteolytic cascade promoting periodontal tissue breakdown, fibrinolysis and bleeding, complement activation, and alveolar bone loss (see "Discussion"). This provides the pathogen with a source of nutrients in the form of tissue breakdown products and hemin, contributing to its colonization and virulence, as well as promoting PD. In cells that express uPAR and plasminogen receptors (*e.g.* macrophages), RgpA-Kgp complex activation of the uPA/plasminogen pathway occurs at the cell surface to promote pericellular proteolysis of the extracellular matrix. RgpA-Kgp-induced activation of uPA at the cell surface may also promote uPA-uPAR signaling, which is known to play a role in cell adhesion, survival, and motility (4).

plasmin activity could confer a significant survival advantage, allowing it to generate nutrients locally and enable it to survive deep in the periodontal pocket (25) (Fig. 7). Indeed, studies have shown that the highest cell numbers of *P. gingivalis* are found in the deepest periodontal pockets (57). Like many other pathogens, *P. gingivalis* has a strict requirement for hemin (18), and the well documented fibrinolytic activity of plasmin would be expected to promote bleeding and enhance its ability to acquire hemin. The ability to access hemin is directly linked to *P. gingivalis* virulence (Fig. 7) (58). Plasmin can degrade both the non-collagenous components (59) via activation of latent metalloproteinases and the collagenous components (1) of gingival tissue and bone matrix, which may also help to explain the protection of $uPA^{-/-}$ mice from *P. gingivalis*-induced bone loss (Fig. 7) (29). It should be noted that there are other oral bacterial species that possess enzymes with trypsin-like activity. For example, *Treponema denticola* has a chymotrypsin-like proteinase (60, 61). Despite its expression of chymotrypsin-like proteinase, we found that inoculation of mice with *T. denticola* alone failed to induce alveolar bone loss in a murine PD model (62). Relatedly, the discovery that apparently innocuous oral commensals were capable of inducing plasmin activity (via streptokinase) (63) suggests that plasmin activity *per se* may not contribute to virulence but might act as a general bacterial sur-

vival strategy. As discussed above, for macrophages the gingipain complex is likely to be acting in close proximity to the cell surface uPAR-uPA and plasminogen receptors (*e.g.* Plg-R_{KT}). In this context, any cell-bound plasmin generated would be largely protected from its inhibitor α2-antiplasmin (64), enabling the enhancement, for example, of macrophage matrix destruction.

We show here that *P. gingivalis*-derived RgpA-Kgp complex specifically targets and activates the uPA/plasminogen pathway. Given the nature of the diverse downstream effector pathways that can be activated by the uPA/plasminogen pathway, including tissue breakdown and fibrinolysis, its activation by *P. gingivalis* would provide it with a significant survival advantage and helps explain its role as a keystone pathogen.

References

1. Carmeliet, P., Moons, L., Lijnen, R., Baes, M., Lemaître, V., Tipping, P., Drew, A., Eeckhout, Y., Shapiro, S., Lupu, F., and Collen, D. (1997) Urokinase-generated plasmin activates matrix metalloproteinases during aneurysm formation. *Nat. Genet.* **17,** 439–444
2. Andreasen, P. A., Egelund, R., and Petersen, H. H. (2000) The plasminogen activation system in tumor growth, invasion, and metastasis. *Cell Mol. Life Sci.* **57,** 25–40
3. Danø, K., Behrendt, N., Høyer-Hansen, G., Johnsen, M., Lund, L. R., Ploug, M., and Rømer, J. (2005) Plasminogen activation and cancer. *Thromb. Haemost.* **93,** 676–681
4. Smith, H. W., and Marshall, C. J. (2010) Regulation of cell signalling by uPAR. *Nat. Rev. Mol. Cell Biol.* **11,** 23–36
5. Hamilton, J. A., Campbell, I. K., Wojta, J., and Cheung, D. (1992) Plasminogen activators and their inhibitors in arthritic disease. *Ann. N.Y. Acad. Sci.* **667,** 87–100
6. Busso, N., Péclat, V., So, A., and Sappino, A. P. (1997) Plasminogen activation in synovial tissues: differences between normal, osteoarthritis, and rheumatoid arthritis joints. *Ann. Rheum. Dis.* **56,** 550–557
7. Busso, N., and Hamilton, J. A. (2002) Extravascular coagulation and the plasminogen activator/plasmin system in rheumatoid arthritis. *Arthritis. Rheum.* **46,** 2268–2279
8. Fleetwood, A. J., Achuthan, A., Schultz, H., Nansen, A., Almholt, K., Usher, P., and Hamilton, J. A. (2014) Urokinase plasminogen activator is a central regulator of macrophage three-dimensional invasion, matrix degradation, and adhesion. *J. Immunol.* **192,** 3540–3547
9. Cook, A. D., Braine, E. L., Campbell, I. K., and Hamilton, J. A. (2002) Differing roles for urokinase and tissue-type plasminogen activator in collagen-induced arthritis. *Am. J. Pathol.* **160,** 917–926
10. Cook, A. D., De Nardo, C. M., Braine, E. L., Turner, A. L., Vlahos, R., Way, K. J., Beckman, S. K., Lenzo, J. C., and Hamilton, J. A. (2010) Urokinase-type plasminogen activator and arthritis progression: role in systemic disease with immune complex involvement. *Arthritis Res. Ther.* **12,** R37
11. Danø, K., Andreasen, P. A., Grøndahl-Hansen, J., Kristensen, P., Nielsen, L. S., and Skriver, L. (1985) Plasminogen activators, tissue degradation, and cancer. *Adv. Cancer Res.* **44,** 139–266
12. Belin, D., Vassalli, J. D., Combépine, C., Godeau, F., Nagamine, Y., Reich, E., Kocher, H. P., and Duvoisin, R. M. (1985) Cloning, nucleotide sequencing and expression of cDNAs encoding mouse urokinase-type plasminogen activator. *Eur. J. Biochem.* **148,** 225–232
13. Stoppelli, M. P., Corti, A., Soffientini, A., Cassani, G., Blasi, F., and Assoian, R. K. (1985) Differentiation-enhanced binding of the amino-terminal fragment of human urokinase plasminogen activator to a specific receptor on U937 monocytes. *Proc. Natl. Acad. Sci. U.S.A.* **82,** 4939–4943
14. Robbins, K. C., and Summaria, L. (1976) Plasminogen and plasmin. *Methods Enzymol.* **45,** 257–273
15. Ellis, V., Scully, M. F., and Kakkar, V. V. (1989) Plasminogen activation initiated by single-chain urokinase-type plasminogen activator. Potentiation by U937 monocytes. *J. Biol. Chem.* **264,** 2185–2188
16. Page, R. C. (1991) The role of inflammatory mediators in the pathogenesis of periodontal disease. *J. Periodontal Res.* **26,** 230–242
17. Chapple, C. C., Srivastava, M., and Hunter, N. (1998) Failure of macrophage activation in destructive periodontal disease. *J. Pathol.* **186,** 281–286
18. Lamont, R. J., and Jenkinson, H. F. (1998) Life below the gum line: pathogenic mechanisms of *Porphyromonas gingivalis*. *Microbiol. Mol. Biol. Rev.* **62,** 1244–1263
19. Socransky, S. S., Haffajee, A. D., Cugini, M. A., Smith, C., and Kent, R. L., Jr. (1998) Microbial complexes in subgingival plaque. *J. Clin. Periodontol.* **25,** 134–144
20. Hajishengallis, G., Liang, S., Payne, M. A., Hashim, A., Jotwani, R., Eskan, M. A., McIntosh, M. L., Alsam, A., Kirkwood, K. L., Lambris, J. D., Darveau, R. P., and Curtis, M. A. (2011) Low-abundance biofilm species orchestrates inflammatory periodontal disease through the commensal microbiota and complement. *Cell Host Microbe* **10,** 497–506
21. Darveau, R. P., Hajishengallis, G., and Curtis, M. A. (2012) *Porphyromonas gingivalis* as a potential community activist for disease. *J. Dent. Res.* **91,** 816–820
22. Imamura, T. (2003) The role of gingipains in the pathogenesis of periodontal disease. *J. Periodontol.* **74,** 111–118
23. Rajapakse, P. S., O'Brien-Simpson, N. M., Slakeski, N., Hoffmann, B., and Reynolds, E. C. (2002) Immunization with the RgpA-Kgp proteinase-adhesin complexes of *Porphyromonas gingivalis* protects against periodontal bone loss in the rat periodontitis model. *Infect. Immun.* **70,** 2480–2486
24. O'Brien-Simpson, N. M., Pathirana, R. D., Paolini, R. A., Chen, Y. Y., Veith, P. D., Tam, V., Ally, N., Pike, R. N., and Reynolds, E. C. (2005) An immune response directed to proteinase and adhesin functional epitopes protects against *Porphyromonas gingivalis*-induced periodontal bone loss. *J. Immunol.* **175,** 3980–3989
25. Bostanci, N., and Belibasakis, G. N. (2012) *Porphyromonas gingivalis*: an invasive and evasive opportunistic oral pathogen. *FEMS Microbiol. Lett.* **333,** 1–9
26. Pinchback, J. S., Gibbins, J. R., and Hunter, N. (1996) Vascular co-localization of proteolytic enzymes and proteinase inhibitors in advanced periodontitis. *J. Pathol.* **179,** 326–332
27. Brown, J. M., Watanabe, K., Cohen, R. L., and Chambers, D. A. (1995) Molecular characterization of plasminogen activators in human gingival crevicular fluid. *Arch. Oral Biol.* **40,** 839–845
28. DeCarlo, A. A., Grenett, H., Park, J., Balton, W., Cohen, J., and Hardigan, P. (2007) Association of gene polymorphisms for plasminogen activators with alveolar bone loss. *J. Periodontal Res.* **42,** 305–310
29. Lam, R. S., O'Brien-Simpson, N. M., Hamilton, J. A., Lenzo, J. C., Holden, J. A., Brammar, G. C., Orth, R. K., Tan, Y., Walsh, K. A., Fleetwood, A. J., and Reynolds, E. C. (2015) GM-CSF and uPA are required for *Porphyromonas gingivalis*-induced alveolar bone loss in a mouse periodontitis model. *Immunol Cell Biol.* 10.1038/icb.2015.25
30. Hamilton, J. A., Vairo, G., Knight, K. R., and Cocks, B. G. (1991) Activation and proliferation signals in murine macrophages. Biochemical signals controlling the regulation of macrophage urokinase-type plasminogen activator activity by colony-stimulating factors and other agents. *Blood* **77,** 616–627
31. Lam, R. S., O'Brien-Simpson, N. M., Lenzo, J. C., Holden, J. A., Brammar, G. C., Walsh, K. A., McNaughtan, J. E., Rowler, D. K., Van Rooijen, N., and Reynolds, E. C. (2014) Macrophage depletion abates *Porphyromonas gingivalis*-induced alveolar bone resorption in mice. *J. Immunol.* **193,** 2349–2362
32. Fleetwood, A. J., Lawrence, T., Hamilton, J. A., and Cook, A. D. (2007) Granulocyte-macrophage colony-stimulating factor (CSF) and macrophage CSF-dependent macrophage phenotypes display differences in cytokine profiles and transcription factor activities: implications for CSF blockade in inflammation. *J. Immunol.* **178,** 5245–5252
33. Lund, I. K., Jögi, A., Rønø, B., Rasch, M. G., Lund, L. R., Almholt, K., Gårdsvoll, H., Behrendt, N., Rømer, J., and Høyer-Hansen, G. (2008) Antibody-mediated targeting of the urokinase-type plasminogen activator proteolytic function neutralizes fibrinolysis *in vivo*. *J. Biol. Chem.* **283,** 32506–32515
34. O'Brien-Simpson, N. M., Black, C. L., Bhogal, P. S., Cleal, S. M., Slakeski, N., Higgins, T. J., and Reynolds, E. C. (2000) Serum immunoglobulin G

(IgG) and IgG subclass responses to the RgpA-Kgp proteinase-adhesin complex of *Porphyromonas gingivalis* in adult periodontitis. *Infect Immun* **68,** 2704–2712
35. Pathirana, R. D., O'Brien-Simpson, N. M., Veith, P. D., Riley, P. F., and Reynolds, E. C. (2006) Characterization of proteinase-adhesin complexes of *Porphyromonas gingivalis*. *Microbiology* **152,** 2381–2394
36. Lacey, D. C., Achuthan, A., Fleetwood, A. J., Dinh, H., Roiniotis, J., Scholz, G. M., Chang, M. W., Beckman, S. K., Cook, A. D., and Hamilton, J. A. (2012) Defining GM-CSF- and macrophage-CSF-dependent macrophage responses by in vitro models. *J. Immunol.* **188,** 5752–5765
37. Chen, Y. Y., Peng, B., Yang, Q., Glew, M. D., Veith, P. D., Cross, K. J., Goldie, K. N., Chen, D., O'Brien-Simpson, N., Dashper, S. G., and Reynolds, E. C. (2011) The outer membrane protein LptO is essential for the *O*-deacylation of LPS and the co-ordinated secretion and attachment of A-LPS and CTD proteins in *Porphyromonas gingivalis*. *Mol. Microbiol.* **79,** 1380–1401
38. Wells, J. M., and McLuckey, S. A. (2005) Collision-induced dissociation (CID) of peptides and proteins. *Methods Enzymol.* **402,** 148–185
39. Birkedal-Hansen, H. (1993) Role of matrix metalloproteinases in human periodontal diseases. *J. Periodontol.* **64,** 474–484
40. Castellino, F. J., and Ploplis, V. A. (2005) Structure and function of the plasminogen/plasmin system. *Thromb. Haemost.* **93,** 647–654
41. Gaffen, S. L., and Hajishengallis, G. (2008) A new inflammatory cytokine on the block: re-thinking periodontal disease and the Th1/Th2 paradigm in the context of Th17 cells and IL-17. *J. Dent. Res.* **87,** 817–828
42. Schuliga, M., Westall, G., Xia, Y., and Stewart, A. G. (2013) The plasminogen activation system: new targets in lung inflammation and remodeling. *Curr. Opin. Pharmacol.* **13,** 386–393
43. Koziel, J., Mydel, P., and Potempa, J. (2014) The link between periodontal disease and rheumatoid arthritis: an updated review. *Curr. Rheumatol. Rep.* **16,** 408
44. Falcone, D. J., Borth, W., Khan, K. M., and Hajjar, K. A. (2001) Plasminogen-mediated matrix invasion and degradation by macrophages is dependent on surface expression of annexin II. *Blood* **97,** 777–784
45. Miles, L. A., Lighvani, S., Baik, N., Parmer, C. M., Khaldoyanidi, S., Mueller, B. M., and Parmer, R. J. (2014) New insights into the role of Plg-RKT in macrophage recruitment. *Int. Rev. Cell Mol. Biol.* **309,** 259–302
46. McAlister, A. D., Sroka, A., Fitzpatrick, R. E., Quinsey, N. S., Travis, J., Potempa, J., and Pike, R. N. (2009) Gingipain enzymes from *Porphyromonas gingivalis* preferentially bind immobilized extracellular proteins: a mechanism favouring colonization? *J. Periodontal Res.* **44,** 348–353
47. Singh, B., Su, Y. C., and Riesbeck, K. (2010) Vitronectin in bacterial pathogenesis: a host protein used in complement escape and cellular invasion. *Mol. Microbiol.* **78,** 545–560
48. Félez, J., Miles, L. A., Fábregas, P., Jardí, M., Plow, E. F., and Lijnen, R. H. (1996) Characterization of cellular binding sites and interactive regions within reactants required for enhancement of plasminogen activation by tPA on the surface of leukocytic cells. *Thromb. Haemost.* **76,** 577–584
49. Andronicos, N. M., Chen, E. I., Baik, N., Bai, H., Parmer, C. M., Kiosses, W. B., Kamps, M. P., Yates, J. R., 3rd, Parmer, R. J., and Miles, L. A. (2010) Proteomics-based discovery of a novel, structurally unique, and developmentally regulated plasminogen receptor, Plg-RKT, a major regulator of cell surface plasminogen activation. *Blood* **115,** 1319–1330
50. Bharadwaj, A., Bydoun, M., Holloway, R., and Waisman, D. (2013) Annexin A2 heterotetramer: structure and function. *Int. J. Mol. Sci.* **14,** 6259–6305
51. Petersen, H. H., Hansen, M., Schousboe, S. L., and Andreasen, P. A. (2001) Localization of epitopes for monoclonal antibodies to urokinase-type plasminogen activator: relationship between epitope localization and effects of antibodies on molecular interactions of the enzyme. *Eur. J. Biochem.* **268,** 4430–4439
52. Amara, U., Rittirsch, D., Flierl, M., Bruckner, U., Klos, A., Gebhard, F., Lambris, J. D., and Huber-Lang, M. (2008) Interaction between the coagulation and complement system. *Adv. Exp. Med. Biol.* **632,** 71–79
53. Abe, T., Hosur, K. B., Hajishengallis, E., Reis, E. S., Ricklin, D., Lambris, J. D., and Hajishengallis, G. (2012) Local complement-targeted intervention in periodontitis: proof-of-concept using a C5a receptor (CD88) antagonist. *J. Immunol.* **189,** 5442–5448
54. Pathirana, R. D., O'Brien-Simpson, N. M., Brammar, G. C., Slakeski, N., and Reynolds, E. C. (2007) Kgp and RgpB, but not RgpA, are important for *Porphyromonas gingivalis* virulence in the murine periodontitis model. *Infect. Immun.* **75,** 1436–1442
55. Nusrat, A. R., and Chapman, H. A., Jr. (1991) An autocrine role for urokinase in phorbol ester-mediated differentiation of myeloid cell lines. *J. Clin. Invest.* **87,** 1091–1097
56. Kalbasi Anaraki, P., Patecki, M., Tkachuk, S., Kiyan, Y., Haller, H., and Dumler, I. (2015) Urokinase receptor mediates osteoclastogenesis via M-CSF release from osteoblasts and the c-Fms/PI3K/Akt/NF-κB pathway in osteoclasts. *J. Bone Miner. Res.* **30,** 379–388
57. Socransky, S. S., and Haffajee, A. D. (2005) Periodontal microbial ecology. *Periodontol 2000* **38,** 135–187
58. McKee, A. S., McDermid, A. S., Baskerville, A., Dowsett, A. B., Ellwood, D. C., and Marsh, P. D. (1986) Effect of hemin on the physiology and virulence of Bacteroides gingivalis W50. *Infect. Immun.* **52,** 349–355
59. Daci, E., Everts, V., Torrekens, S., Van Herck, E., Tigchelaar-Gutterr, W., Bouillon, R., and Carmeliet, G. (2003) Increased bone formation in mice lacking plasminogen activators. *J. Bone Miner. Res.* **18,** 1167–1176
60. Loesche, W. J., Bretz, W. A., Kerschensteiner, D., Stoll, J., Socransky, S. S., Hujoel, P., and Lopatin, D. E. (1990) Development of a diagnostic test for anaerobic periodontal infections based on plaque hydrolysis of benzoyl-DL-arginine-naphthylamide. *J. Clin. Microbiol.* **28,** 1551–1559
61. Bamford, C. V., Fenno, J. C., Jenkinson, H. F., and Dymock, D. (2007) The chymotrypsin-like protease complex of *Treponema denticola* ATCC 35405 mediates fibrinogen adherence and degradation. *Infect. Immun.* **75,** 4364–4372
62. Orth, R. K., O'Brien-Simpson, N. M., Dashper, S. G., and Reynolds, E. C. (2011) Synergistic virulence of *Porphyromonas gingivalis* and *Treponema denticola* in a murine periodontitis model. *Mol. Oral Microbiol.* **26,** 229–240
63. Kinnby, B., Booth, N. A., and Svensäter, G. (2008) Plasminogen binding by oral streptococci from dental plaque and inflammatory lesions. *Microbiology* **154,** 924–931
64. Plow, E. F., Freaney, D. E., Plescia, J., and Miles, L. A. (1986) The plasminogen system and cell surfaces: evidence for plasminogen and urokinase receptors on the same cell type. *J. Cell Biol.* **103,** 2411–2420

Porphyromonas gingivalis-derived RgpA-Kgp Complex Activates the Macrophage Urokinase Plasminogen Activator System: IMPLICATIONS FOR PERIODONTITIS

Andrew J. Fleetwood, Neil M. O'Brien-Simpson, Paul D. Veith, Roselind S. Lam, Adrian Achuthan, Andrew D. Cook, William Singleton, Ida K. Lund, Eric C. Reynolds and John A. Hamilton

J. Biol. Chem. 2015, 290:16031-16042.
doi: 10.1074/jbc.M115.645572 originally published online May 15, 2015

Author/s:
Fleetwood, AJ; O'Brien-Simpson, NM; Veith, PD; Lam, RS; Achuthan, A; Cook, AD; Singleton, W; Lund, IK; Reynolds, EC; Hamilton, JA

Title:
Porphyromonas gingivalis-derived RgpA-Kgp Complex Activates the Macrophage Urokinase Plasminogen Activator System IMPLICATIONS FOR PERIODONTITIS

Date:
2015-06-26

Citation:
Fleetwood, A. J., O'Brien-Simpson, N. M., Veith, P. D., Lam, R. S., Achuthan, A., Cook, A. D., Singleton, W., Lund, I. K., Reynolds, E. C. & Hamilton, J. A. (2015). Porphyromonas gingivalis-derived RgpA-Kgp Complex Activates the Macrophage Urokinase Plasminogen Activator System IMPLICATIONS FOR PERIODONTITIS. JOURNAL OF BIOLOGICAL CHEMISTRY, 290 (26), pp.16031-16042. https://doi.org/10.1074/jbc.M115.645572.